

## Supplementary Materials for

### Adult rat myelin enhances axonal outgrowth from neural stem cells

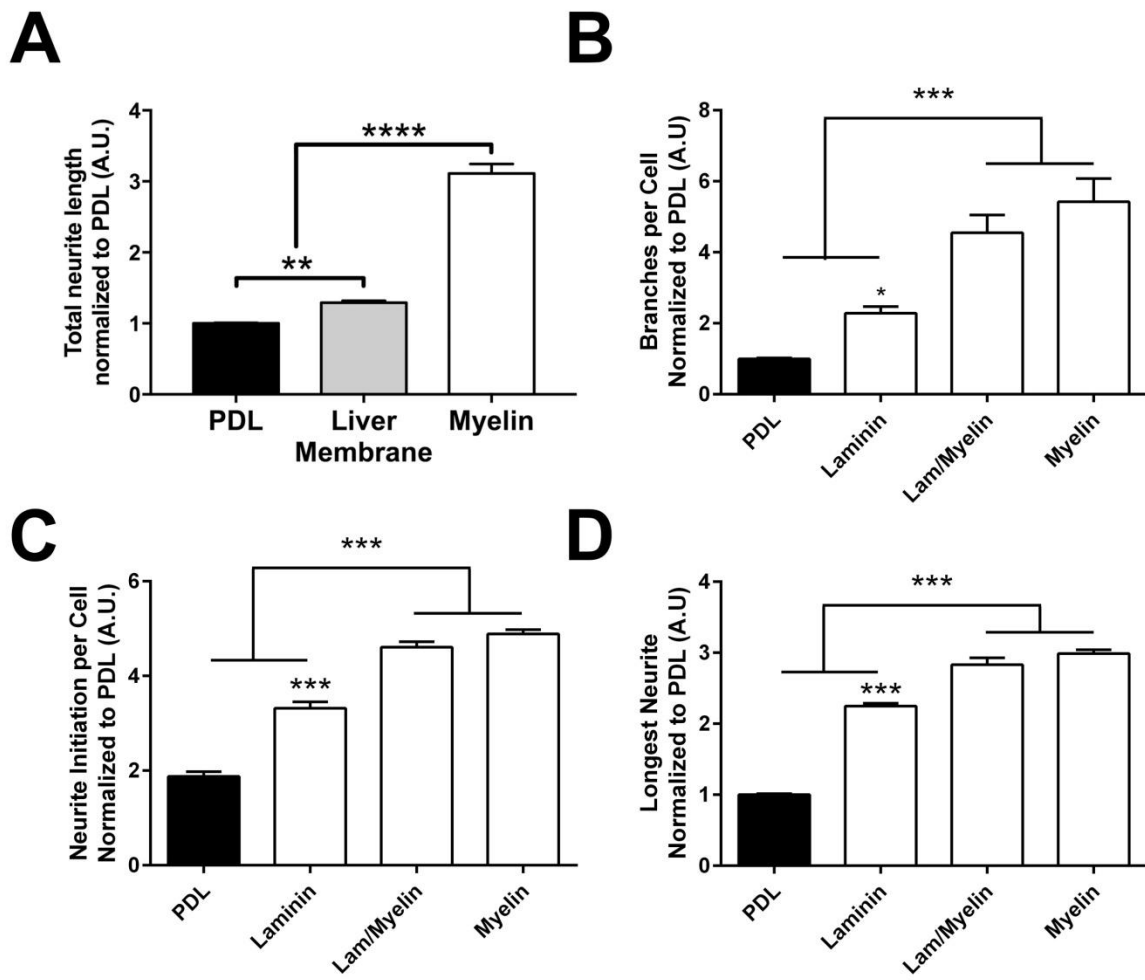
Gunnar H. D. Poplawski, Richard Lie, Matt Hunt, Hiromi Kumamaru, Riki Kawaguchi, Paul Lu, Michael K. E. Schäfer, Grace Woodruff, Jacob Robinson, Philip Canete, Jennifer N. Dulin, Cedric G. Geoffroy, Lutz Menzel, Binhai Zheng, Giovanni Coppola, Mark H. Tuszynski\*

\*Corresponding author. Email: mtuszynski@ucsd.edu

Published 23 May 2018, *Sci. Transl. Med.* **10**, eaal2563 (2018)  
DOI: 10.1126/scitranslmed.aal2563

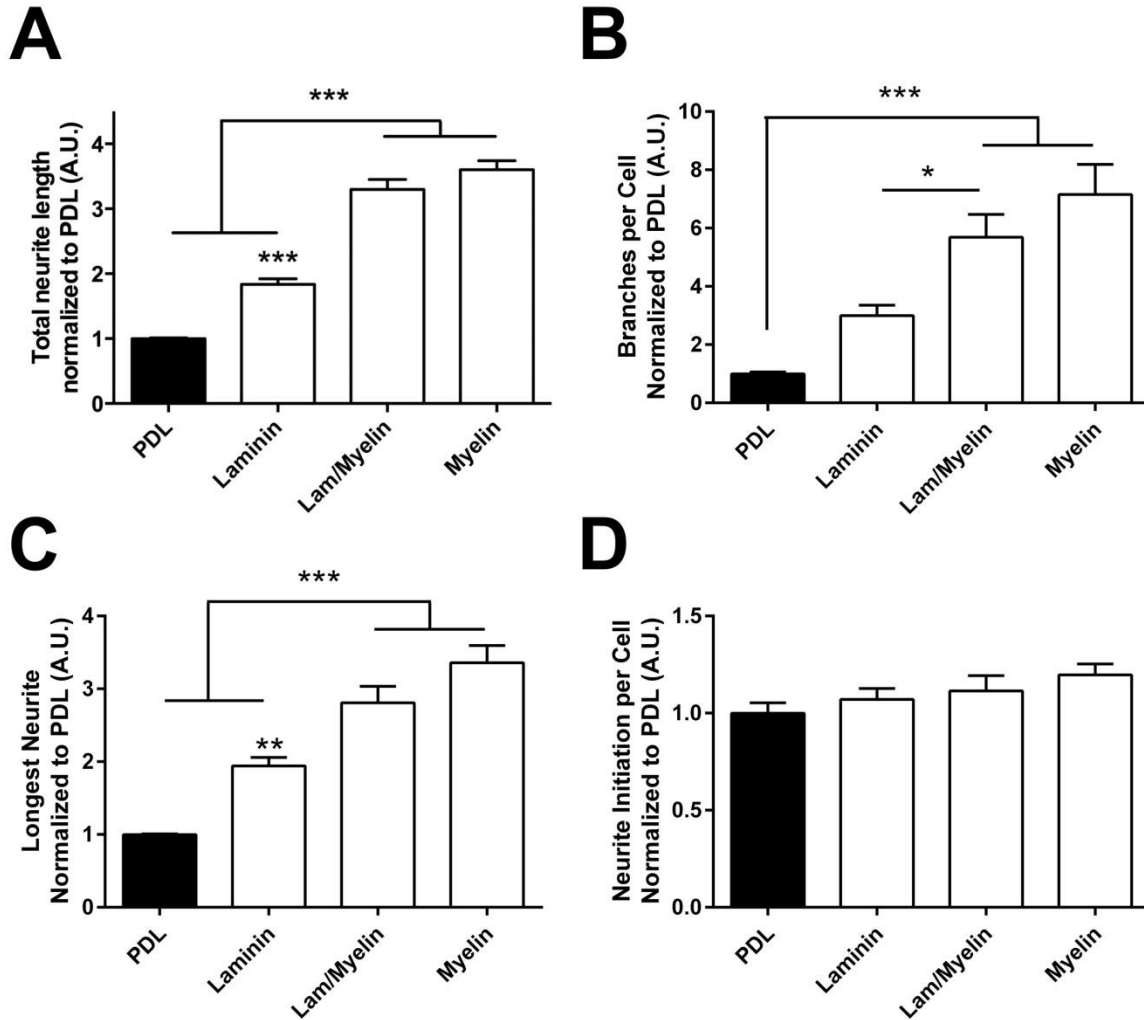
#### This PDF file includes:

- Fig. S1. NPC-derived axon growth is stimulated by a myelin substrate in vitro.
- Fig. S2. Mouse E12 spinal cord-derived NPC neurite growth is stimulated by a myelin substrate in vitro.
- Fig. S3. Axon (Tau1) growth is stimulated by a myelin substrate in vitro.
- Fig. S4. E14 rat spinal cord-derived NPCs lose their ability to be stimulated by myelin upon in vitro maturation.
- Fig. S5. Growth-dependent mechanisms involving pERK.
- Fig. S6. Quality measures of RNA-seq.
- Fig. S7. qPCR verification of RNA-seq.
- Fig. S8. Overexpression of Negr1 in mature spinal cord-derived NPCs increases neurite growth on a myelin substrate in vitro.
- Table S1. Individual level data for experiments with  $n < 20$ .



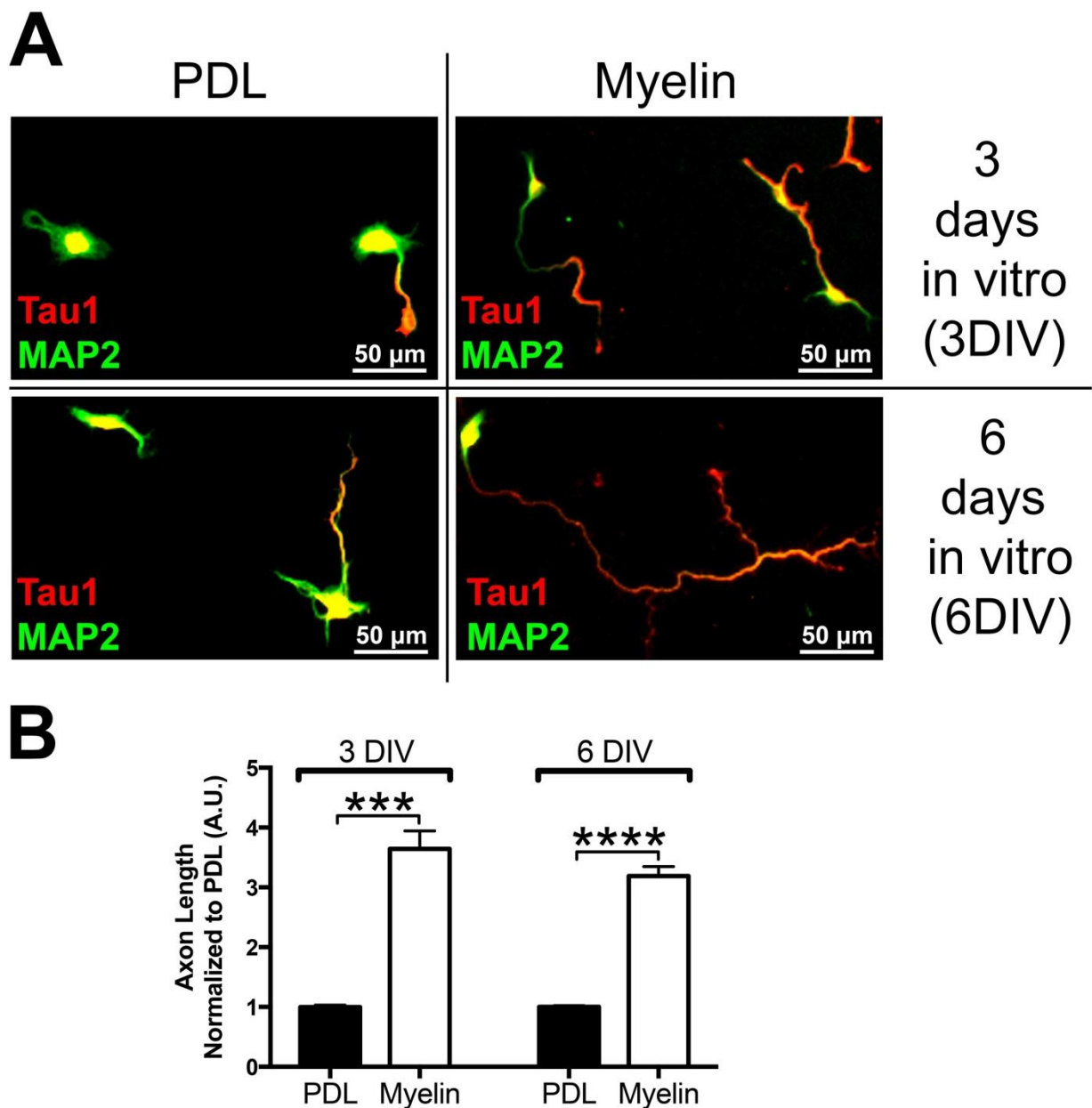
**Figure S1: NPC-derived axon growth is stimulated by a myelin substrate in vitro.**

Enhanced neurite outgrowth ( $\beta$ III-tubulin label) from rat E14 spinal cord-derived NPCs on myelin substrates after 48 hours in vitro. (A) Neurite outgrowth stimulation comparing non-specific membranes from liver tissue to myelin membranes, (B) Neurite branching, (C) neurite initiation per cell, (D) longest neurite. All values are normalized to the PDL condition for each individual experiment. Show are Mean  $\pm$  SEM; \*\*\* $p < 0.001$  One-way ANOVA, with \* $p < 0.05$ , \*\* $p < 0.01$ , \*\*\* $p < 0.001$ , \*\*\*\* $p < 0.0001$ , post-hoc Tukey's;  $n = 3$  embryos,  $n = 4$  wells per embryo.



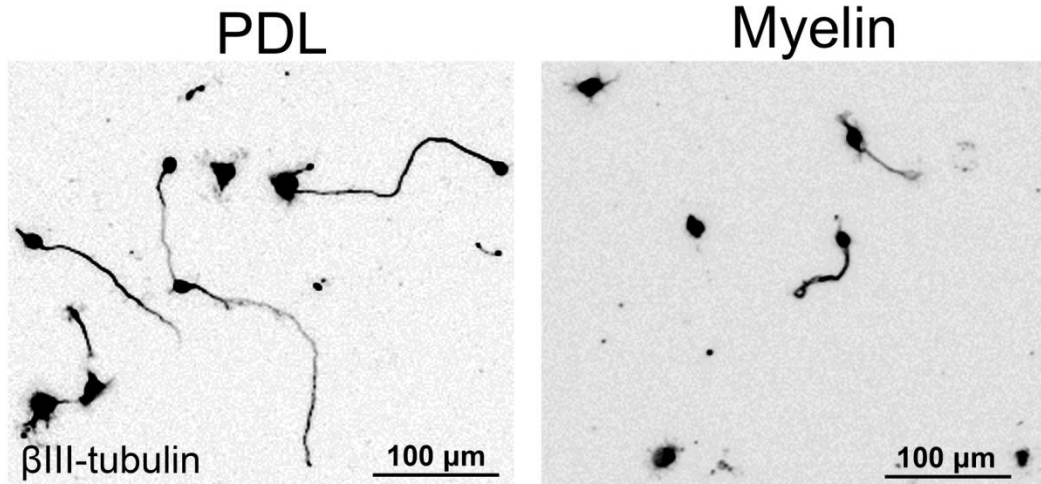
**Figure S2: Mouse E12 spinal cord–derived NPC neurite growth is stimulated by a myelin substrate in vitro.**

Enhanced neurite outgrowth ( $\beta$ III-tubulin label) from mouse E12 spinal cord-derived NPCs on myelin substrates after 48 hours in vitro. (A) Neurite length per cell, (B) Neurite branching per cell, (C) longest neurite and (D) neurite initiation. All values are normalized to the PDL condition for each individual experiment. Show are Mean  $\pm$  SEM; \*\*\* $p < 0.001$  One-way ANOVA, with \* $p < 0.05$ , \*\* $p < 0.01$ , \*\*\* $p < 0.001$ , post-hoc Tukey's;  $n = 3$  embryos,  $n = 4$  wells per embryo

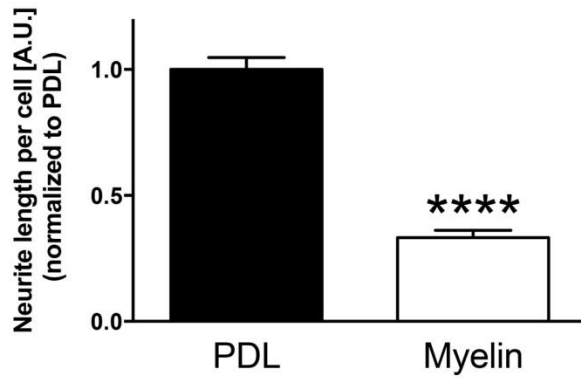
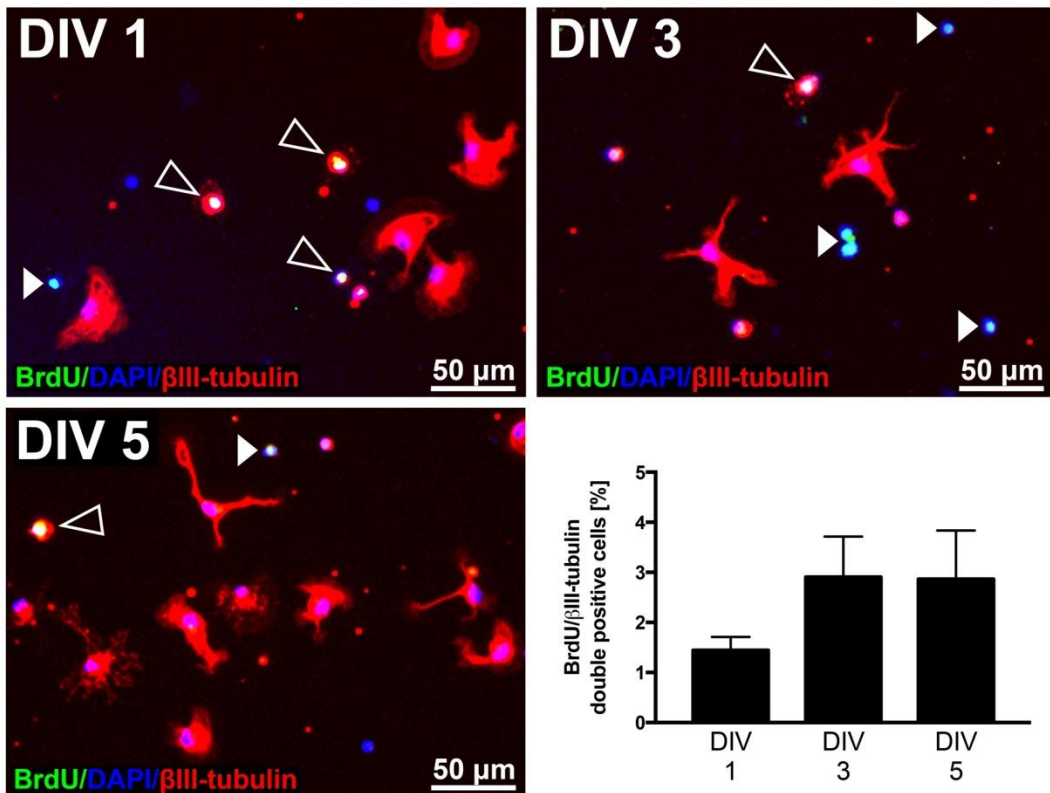


**Figure S3: Axon (Tau1) growth is stimulated by a myelin substrate in vitro.**

(A-D) E14 spinal cord-derived NPCs exhibit stimulation of *axon* growth on myelin substrates identified by the axonal marker Tau1 and the dendritic marker MAP2 after 3 and 6 days in vitro (DIV). (B) Quantification of axonal growth stimulation via Tau1 labeling. Values are normalized to the PDL condition for each individual experiment. Show are Mean  $\pm$  SEM; \*\*\* $p < 0.001$ , \*\*\*\* $p < 0.0001$ , two-tailed t-test;  $n = 3$  embryos,  $n = 4$  wells per embryo. Scale bar: A-D, 100  $\mu\text{m}$ .

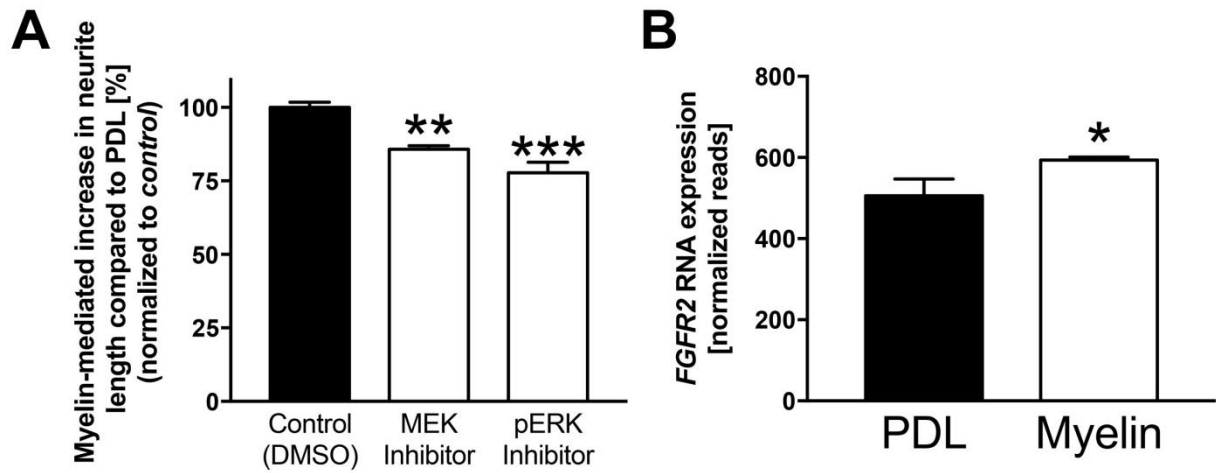
**A**

Replated  
after 6 day  
maturation  
in vitro

**B**

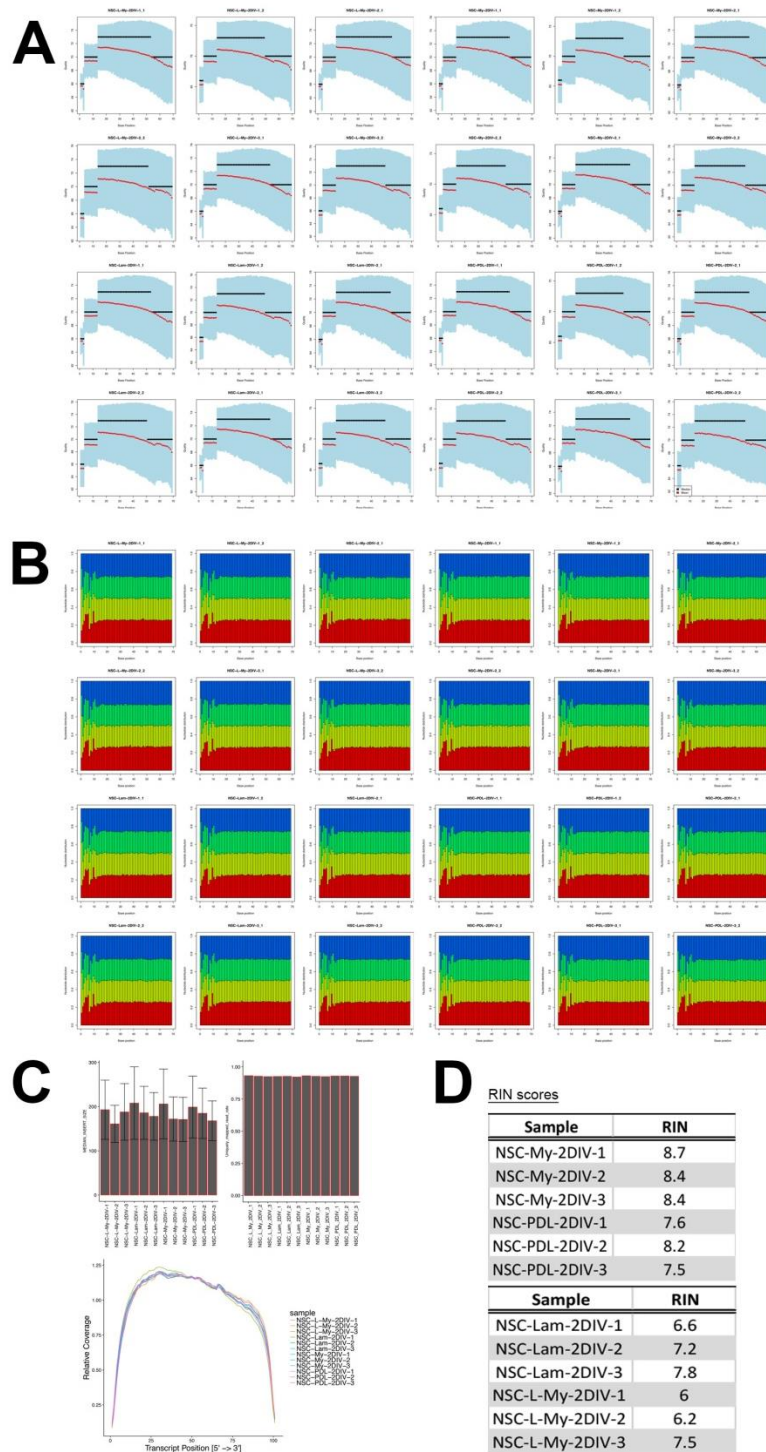
**Figure S4: E14 rat spinal cord–derived NPCs lose their ability to be stimulated by myelin upon in vitro maturation.**

**(A)** E14 spinal cord-derived NPCs were cultured on PDL and matured for 6 days in vitro (6DIV), paralleling the developmental timeframe from E14 to E20. After trypsinization and replating, in vitro “matured” NPCs show significant neurite outgrowth inhibition on myelin compared to PDL substrates. Values are normalized to the PDL condition for each individual experiment (\*\*\*\* $p < 0.0001$ , two-tailed t-test;  $n = 3$  individual experiments). **(B)** E14 spinal cord-derived NPCs were cultured on PDL and fixed after 1, 3 and 5 days in vitro. **BrdU** was added to the culture medium at time of plating to label nuclei that underwent mitosis during the culture period. The nuclear label **DAPI** was used to label all cells in culture and the neuronal marker, and  **$\beta$ III-tubulin** was used to identify the neuronal population. Non-neuronal cells that underwent mitosis co-label for **DAPI** and **BrdU** (white arrowheads) and neuronal cells that underwent mitosis co-label for **DAPI** and **BrdU** and  **$\beta$ III-tubulin** (black arrowheads). Quantification shows that fewer than 3% of cells labeled for BrdU were neuronal ( $n = 3$  embryos,  $n = 3$  wells per embryo). Mean  $\pm$  SEM. Scale bar: A, 100  $\mu$ m; B, 50  $\mu$ m.



**Figure S5: Growth-dependent mechanisms involving *pERK*.**

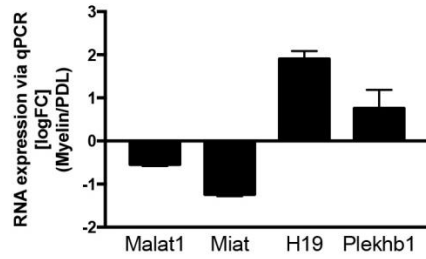
**(A)** Rat E14 spinal cord-derived NPCs were plated on PDL and myelin substrates and cultured in the presence of DMSO (control), ERK-kinase-(MEK)-inhibitor (10  $\mu\text{g/ml}$ ; PD98059) or ERK-inhibitor (12.5  $\mu\text{M}$ ; CAS1049738) for 24 hours. Both inhibitors showed partial blockade (14% and 22%, respectively) of myelin-mediated stimulation compared to DMSO, indicating that *pErk* is an essential, but partial contributor to the stimulatory effects of myelin. Values are normalized to the PDL condition for each individual experiment (\*\*\* $p < 0.001$ , one-way ANOVA, with \*\* $p < 0.01$ , \*\*\* $p < 0.001$  post-hoc Tukey's;  $n = 4$  individual experiments). Mean  $\pm$  SEM. **(B)** *FGFR2*, which has been reported to potentially mediate Negr1-dependent activation of *pERK* (29), is significantly increased upon myelin stimulation as shown by RNA-seq. ( $p = 0.05$ , one-tailed t-test;  $n = 3$  individual experiments). Mean  $\pm$  SEM.



**Figure S6: Quality measures of RNA-seq.**

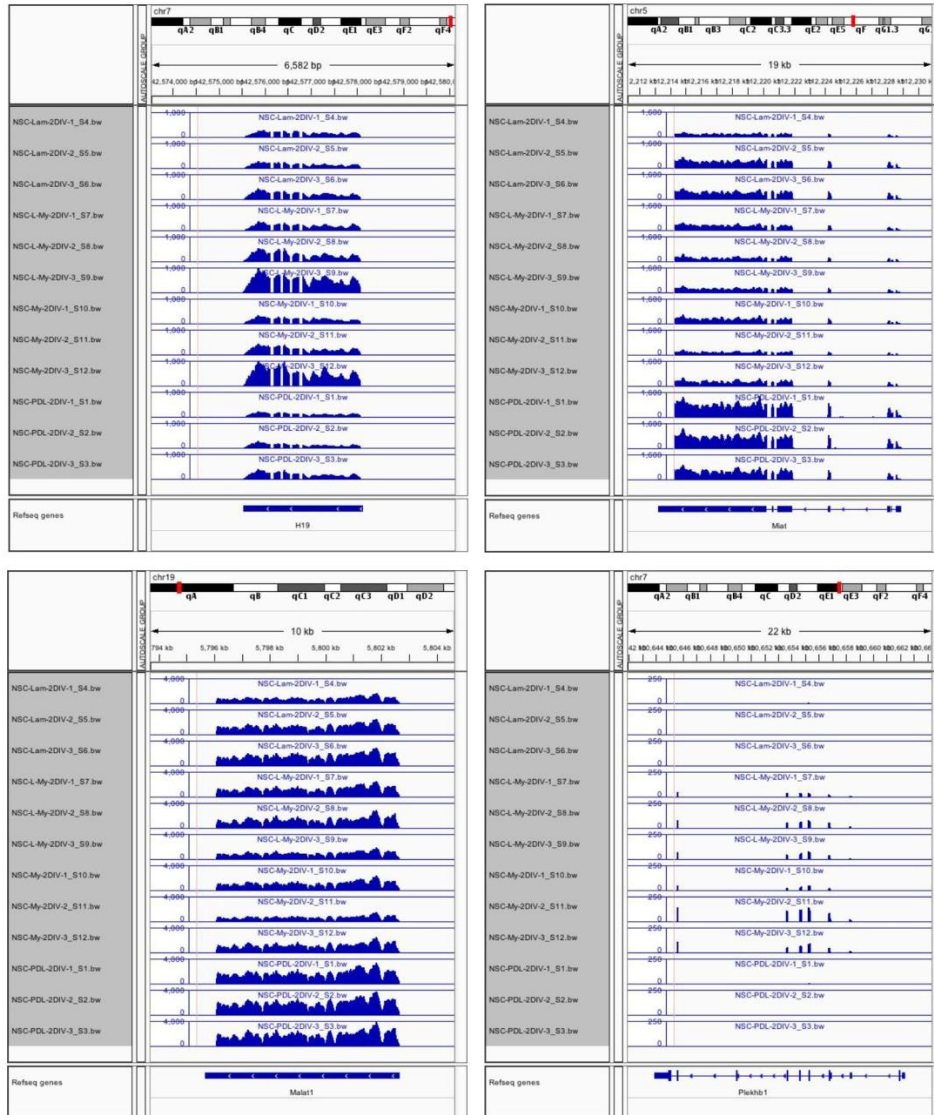
Several measurements showed consistent quality across samples were conducted for consistency of RNA-sequencing data. Consistency of RNA-sequencing quality: **(A)** base quality distribution, **(B)** nucleotide composition, and **(C)** insert sizes, percentage of uniquely aligned reads (>90%) and transcript coverage. Plots in (A) and (B) represent paired-end reads for each sample separately. Error bars in (C) represent  $\pm$  SD. **(D)** RNA integrity number (RIN) for the RNA samples.



**A**

RNAseq Data

Gene name	refSeq	Rank	logFC_Mye_vs_PDL	FDR_Mye_vs_PDL
Malat1	NR_002847	22	-0.903049544	0.00024071
Miat	NR_033657	153	-1.34474975	1.03E-09
H19	NR_001592	2702	0.983220962	0.096013131
Plekhh1	NM_013746	6941	5.603426205	3.45E-33

**B****Figure S7: qPCR verification of RNA-seq.****(A)** qPCR validation of selected differentially expressed genes from RNAseq analysis.Mean  $\pm$  SEM log-2 fold changes, n = 3 individual experiments. **(B)** Integrative Genomics

Viewer (IGV) RNA-seq screenshots for the selected genes.

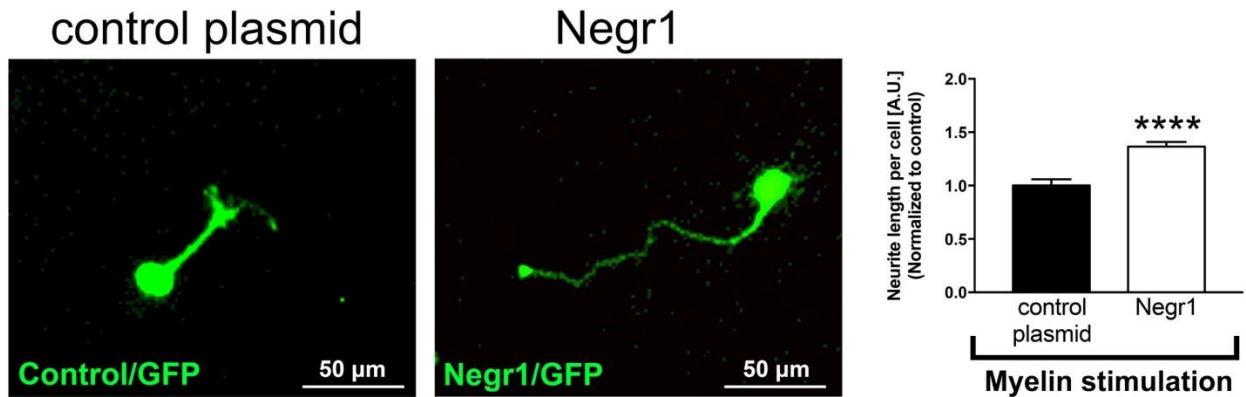


**Figure S8: Overexpression of Negr1 in mature spinal cord-derived NPCs increases neurite growth on a myelin substrate in vitro.**

Rat E14 spinal cord-derived NPCs were co-electroporated with either Negr1-pcDNA3 + Pmax-GFP (Lonza) or with empty pcDNA3 backbone (30) + Pmax-GFP and plated on PDL. After maturation for 6 days in culture, cells were trypsinized, re-plated on myelin substrates, and neurite extension of GFP+ neurons in both conditions was quantified 24 hours later. Values are normalized to the control condition for each individual experiment (\*\*\*\* $p < 0.0001$ , two-tailed t-test;  $n = 3$  individual experiments). Mean  $\pm$  SEM. Scale bar: 100  $\mu\text{m}$ .

**Table S1: Individual level data for experiments with  $n < 20$ .**



Figure S1B				Figure S1C			
PDL	Laminin	Lam/Myelin	Myelin	PDL	Laminin	Lam/Myelin	Myelin
1.036805	2.974649	6.844672	7.446768	1.503185	2.72379	4.464111	4.667819
0.9327578	2.248227	6.511783	8.099982	1.62685	2.733883	4.403545	4.786535
1.030437	3.142875	4.990945	7.958589	1.447552	2.981279	3.996645	4.880961
1.013797	2.531725	4.694995	4.687332	1.877129	3.706865	5.070045	5.035917
1.014571	2.548718	4.732308	5.17731	1.914371	3.578411	4.980132	5.24639
0.9716306	2.103575	4.601326	5.145464	2.172535	3.292302	5.00317	5.336112
0.901384	1.584791	2.914891	3.495752	2.125754	3.531801	4.490929	4.593424
0.965476	1.665377	2.92851	3.216261	2.163162	3.650732	4.522177	4.631714
1.133139	1.769764	2.734036	3.596031	2.089062	3.659744	4.541465	4.828947
Figure S1D				Figure S2A			
PDL	Laminin	Lam/Myelin	Myelin	PDL	Laminin	Lam/Myelin	Myelin
0.968717	2.226842	2.703598	2.784066	1.022281	2.171786	3.252658	3.837268
0.997264	2.072961	2.567502	2.917486	0.9419227	2.6056	3.207879	4.430448
1.03402	2.289064	2.376214	2.813211	1.035796	2.235878	1.618051	2.247527
0.980925	2.274325	3.13499	2.899399	1.027782	2.053363	3.725694	3.578325
1.022243	2.391152	3.19475	3.198653	1.009762	1.834936	3.454604	4.288897
0.996832	2.352504	3.174733	3.15986	0.9624555	1.919756	3.416583	3.878588
0.943506	2.076361	2.819913	3.10993	0.9403325	1.613241	1.911724	2.339585
0.970897	2.211519	2.836121	2.852723	1.011017	1.646502	2.649237	2.999243
1.085597	2.345921	2.692174	3.148058	1.04865	1.701562	2.632786	3.580889
Figure S2B				Figure S2C			
PDL	Laminin	Lam/Myelin	Myelin	PDL	Laminin	Lam/Myelin	Myelin
1.291745	3.407408	7.61128	9.22094	1.039438	2.811903	3.705822	5.111195
0.785278	5.131862	8.130276	11.88669	1.048731	2.072876	4.914915	4.820434
0.922965	3.693468	2.706113	4.847388	0.9118304	2.10251	3.898753	2.501643
1.046447	3.329358	8.183002	7.693183	0.9161535	1.475095	3.146789	3.516952
1.028441	2.736833	7.334257	10.18953	1.030493	1.636621	3.271878	3.703213
0.925108	2.966447	6.603623	8.675414	1.053353	1.628759	3.174637	3.960066
0.766294	1.905429	2.349286	2.974168	1.030644			3.225423
1.33081	2.065459	4.360406	4.388721	0.9397036			3.213254
0.902889	1.736307	3.931937	4.545713	1.029652			3.732923
Figure S2C				Figure S2D			
PDL	Laminin	Lam/Myelin	Myelin	PDL	Laminin	Lam/Myelin	Myelin
1.030357	2.127674	3.020882	3.643303	1.02762	1.594245	3.466608	3.505965
0.962145	2.648937	3.089812	4.161821	0.9723803	1.468289	3.735374	3.974663
1.007497	2.162693	1.753581	2.314597	1.007616	1.494366	3.301108	3.439279
1.028513	2.041152	3.659352	3.673543	0.9923841	1.474494	3.74481	3.547771
1.005079	1.810385	3.4715	4.189525	1.00045	1.377546	3.63923	3.503495
0.966407	1.901218	3.377709	3.743196	0.9995495	1.625126	3.411883	3.535678
Figure S2C				Figure S2D			
PDL	Laminin	Lam/Myelin	Myelin	PDL	Laminin	Lam/Myelin	Myelin
0.981753	1.597459	1.987859	2.409643	0.839159	0.8885576	0.935184	1.00452
1.013891	1.588638	2.469688	2.751496	0.792792	0.9529179	0.88395	1.10002
1.004356	1.596018	2.452187	3.33983	1.368048	1.47329	1.654501	1.50415
				1.014303	1.092331	1.226685	1.115212
				0.992839	1.081372	1.118964	1.287987
				0.992858	1.095168	1.158197	1.272972
				0.966551	1.00353	0.868511	0.997745
				0.998618	0.9832631	1.095006	1.153555
				1.034831	1.06801	1.087719	1.336714
Figure S3							
3div map2 growth (PDL)	3div MAP2 growth (myelin)	3div tau1 growth (PDL)	3div tau1 growth (myelin)	6div map2 growth (PDL)	6div MAP2 growth (myelin)	6div tau1 growth (PDL)	6div tau1 growth (myelin)
0.989969737	1.644371379	0.941470072	4.220923003	0.978846935	1.733180137	0.992810379	3.217336881
1.004221172	1.834989318	1.034257547	3.218849347	1.033590464	1.819612707	0.982711321	3.331300809
1.005809091	1.804107287	1.02427238	3.497064824	0.987562601	1.847605139	1.0244783	3.020434773
Figure S4B				Figure S5A			
% neuronal BrdU of DAPI 1DIV	% neuronal BrdU of DAPI 3DIV	% neuronal BrdU of DAPI 5DIV		increase in neurite length [%] CAS1049738	increase in neurite length [%] DMSO	increase in neurite length [%] PD98059	
1.972872513	1.323043005	1.388888333		73.82872844	103.6300807	87.28094053	
1.223582197	3.953147854	4.702413369		73.72911881	98.66832767	88.02618711	
1.130653272	3.448275862	2.496329515		75.06386814	97.13605546	84.67144505	
				88.39839405	100.5655362	83.25872637	